



<b>Customer</b> : ESRIN	<b>Document Ref</b> : SST_CCI-ATBD-DMI-201
<b>Contract No</b> : 4000109848/13/I-NB	<b>Issue Date</b> : 02 February 2018
<b>WP No</b> : 100	<b>Issue</b> : 1.0


**Project** : SST CCI Phase-II

**Title** : ATBD - DMI Optimal Estimator for PMW SST retrievals

**Abstract** : This document contains the ATBD for WP100 in Phase-II of the SST\_cci project.

**Author(s)** :   
Pia Nielsen-Englyst, Jacob L.  
Høyer, Leif Toudal Pedersen  
and Jörg Steinwagner  
DMI

**Checked by** :   
Chris Merchant  
Science Leader, UoR  
Ruth Wilson  
Assistant PM, SCL

**Accepted by** :  
  
  
Craig Donlon  
ESA Technical Officer  
ESTEC

**Distribution** : SST\_cci team members  
ESA (Craig Donlon)

**EUROPEAN SPACE AGENCY  
CONTRACT REPORT**

The work described in this report was done under ESA contract.  
Responsibility for the contents resides in the author or organisation  
that prepared it.



## **AMENDMENT RECORD**

This document shall be amended by releasing a new edition of the document in its entirety. The Amendment Record Sheet below records the history and issue status of this document.

### **AMENDMENT RECORD SHEET**

<b>ISSUE</b>	<b>DATE</b>	<b>REASON FOR CHANGE</b>
0.1	25-10-17	First draft for internal review
1.0	02-02-18	Issued following internal reviews

## TABLE OF CONTENTS

1.1 Introduction .....	4
1.2 Input data .....	4
1.2.1 Preprocessing .....	5
2.1 The Inverse Problem .....	5
2.2 Forward Model.....	6
2.3 OE set-up .....	6
2.3.1 Iterations .....	7
2.3.2 Bias corrections.....	8
2.3.2 Final configuration .....	8
2.4 Output data .....	9

## 1. Overview and background information

### 1.1 Introduction

The sea surface temperature (SST) is an essential climate variable that is fundamental for climate monitoring and for the understanding of the air-sea interactions. It has been observed from infrared satellites since the early 1980's, but these observations are limited by clouds and severely impacted by aerosols (Vázquez-Cuervo et al., 2004, Reynolds, 1993; Reynolds et al., 2002). SST observations from passive microwave (PMW) observations are widely recognized as an important alternative to the infrared observations (Donlon et al., 2007, Donlon et al., 2009). They are not limited by clouds and the impact of aerosols is small (Wentz et al., 2000; Chelton and Wentz, 2005).

We have used the Optimal Estimation (OE) principle to retrieve PMW SSTs. OE retrieval methodology differs from e.g. standard regression models, in that it utilizes a forward model that includes Numerical Weather Prediction (NWP) information to calculate simulated brightness temperatures. The use of OE for determining SST does incur additional computational costs because of the required forward modeling, but can have significant advantages as the optimal estimator can be designed to account for both retrieval error and SST sensitivity (Merchant et al., 2013). In general, PMW SST retrievals are challenging due to several effects not related to the SST from e.g. wind, atmospheric attenuation and emission, sun-glint, land contamination, and Radio Frequency Interference (RFI). The use of simulations and the OE methodology for the retrieval is therefore tempting as they provide additional information which can be used to filter these effects out.

This algorithm theoretical basis document (ATBD) describes in detail the DMI OE Algorithm for the retrieval of SST from the JAXA's Advanced Microwave Scanning Radiometer - Earth Observing System (AMSR-E) instrument. More information on the OE setup can be found in Nielsen-Englyst et al., 2018.

### 1.2 Input data

The input to the retrieval processor that we are using is a Multisensor Matchup Dataset (MMD), version MMD6c, but the algorithm is designed to work on any dataset that contains the AMSR-E brightness temperature with auxiliary information. The MMD6c dataset consists of simultaneous overpasses of AMSR-E data matched to a large dataset of SST *in situ* measurements. This *in situ* dataset used for the algorithm testing and validation is composed of quality controlled measurements taken from the International Comprehensive Ocean-Atmosphere Dataset (ICOADS) version 2.5.1, the Met Office Hadley Centre Ensembles dataset version 4.2.0 (EN4) (Good et al., 2013) and Global Tropical Moored Buoy Array (GT MBA) data taken from NOAA PMEL (McPhaden et al. 2009).

For the identification of the matchups and the extraction of the data we used the Multisensor Matchup System (MMS) software that has been developed for the ESA SST-CCI project and European Union's Horizon 2020 research and innovation programme under grant agreement No 638822 (FIDUCEO project) (Block et al., 2017). The MMD also includes the ERA-Interim NWP data (Dee et al., 2011) and sea surface salinity (SSS) from the World Ocean Atlas (WOA) 2013 version 2 (Zweng et al., 2013; Boyer et al., 2013) referencing each AMSR-E pixel and each *in situ* measurement. These data were linearly interpolated in time and space to the matchup location.

## 1.2.1 Preprocessing

A number of fields need to be calculated from the MMD. These include the:

- The integrated (columnar) cloud liquid water content (TCLW)  
In order to get TCLW the pressure is calculated from the surface pressure on 60 levels:

$$P = a + b \cdot P_{surf}$$

where the constants  $a$  and  $b$  are given in Table A1. TCLW is then given by

$$TCLW = \text{sum} \left( \frac{clw \cdot dP}{g} \right),$$

where  $dP$  is the pressure difference between two levels,  $g$  is the gravity constant and CLW is the cloud liquid water field from the MMD.

- Wind speed  
The wind speed (WS) is calculated by:

$$WS = \sqrt{u^2 + v^2},$$

where  $u$  and  $v$  are the east and north component of the wind vector.

- Wind direction relative to satellite azimuth,  $\varphi_{REL}$  is calculated by:

$$\varphi_{REL} = \varphi_{SAT} - \varphi_{WD},$$

where  $\varphi_{WD}$  is the direction the wind is blowing towards relative to north and  $\varphi_{SAT}$  is satellite azimuth angle.

## 2. Algorithm description

### 2.1 The Inverse Problem

We use an OE based inversion technique to find the most probable ocean and atmospheric state given AMSR-E measurements and some prior knowledge based on NWP fields. The inversion approach follows the OE technique by Rodgers 2000 and we broadly follow his conventions. The relationship between the geophysical parameters i.e. the state vector  $\mathbf{x}$ , and the corresponding ideal measurement  $\mathbf{y}$ , is determined by the physics of the measurement, which can be described as the forward function  $\mathbf{f}(\mathbf{x})$  (Rodgers 2000):

$$\mathbf{y}_i = \mathbf{f}(\mathbf{x}). \quad (1)$$

In practice, there will always be a measurement error and it will also be necessary to approximate the ideal physics by a forward model approximation  $\mathbf{F}(\mathbf{x})$ . The relationship between the geophysical parameters and the measured brightness temperatures can be generalized to the following expression:

$$\mathbf{y} = \mathbf{F}(\mathbf{x}) + \epsilon, \quad (2)$$

where  $\mathbf{y}$  is the measurement vector (observed microwave brightness temperatures);  $\mathbf{F}(\mathbf{x})$  is the non-linear forward model approximating the physics of the measurement including the radiative transfer through the atmosphere (Wentz and Meissner 2000);  $\mathbf{x}$  is the state vector containing the relevant

geophysical properties of the ocean and atmosphere; and  $e$  is an error term containing uncertainties due to the measurement noise and errors in the forward model. According to Eq. 5.3 of Rodgers (2000) we aim to find the state vector  $\mathbf{x}$ , which minimizes the cost function  $\mathbf{J}$ :

$$\mathbf{J} = [\mathbf{y} - \mathbf{F}(\mathbf{x})]^T \mathbf{S}_\epsilon^{-1} [\mathbf{y} - \mathbf{F}(\mathbf{x})] + (\mathbf{x} - \mathbf{x}_a)^T \mathbf{S}_a^{-1} (\mathbf{x} - \mathbf{x}_a), \quad (4)$$

where  $\mathbf{S}_\epsilon$  is a covariance matrix for the measurement and forward model uncertainties,  $\mathbf{S}_a$  is the covariances of the a priori state  $\mathbf{x}_a$  (the a priori guess of the ocean and atmospheric state  $\mathbf{x}$ ). The cost function,  $\mathbf{J}$ , is a measure of the goodness of the fit to both the measurements (first term on the right) and the a priori state (second term on the right) balanced by the inverse of their relative uncertainties ( $\mathbf{S}_\epsilon$  and  $\mathbf{S}_a$ ).

In this nonlinear case, Newtonian iteration is a straightforward numerical method for finding the zero gradient of the cost function. Using Newtonian iteration, the state  $\mathbf{x}$  that minimizes the cost function can be found by:

$$\mathbf{x}_{i+1} = \mathbf{x}_i + \mathbf{S}_x [\mathbf{K}_i^T \mathbf{S}_\epsilon^{-1} (\mathbf{y} - \mathbf{F}(\mathbf{x}_i)) - \mathbf{S}_a^{-1} (\mathbf{x}_i - \mathbf{x}_a)], \quad (5)$$

where  $\mathbf{S}_x$  is the error covariance matrix of the retrieved parameters:

$$\mathbf{S}_x = (\mathbf{S}_a^{-1} + \mathbf{K}_i^T \mathbf{S}_\epsilon^{-1} \mathbf{K}_i)^{-1}. \quad (6)$$

The matrix  $\mathbf{K}$  expresses the sensitivity of the forward model to a perturbation in the retrieved parameters, i.e. it is a matrix consisting of the partial derivatives of the brightness temperatures in a particular channel with respect to each parameter of the state vector. Due to the non-linearity these partial derivatives need to be computed at each iteration step (state).

The averaging kernel matrix,  $\mathbf{A}$ , relates the sensitivity of the retrieval to the true state. It is defined as:

$$\mathbf{A} = \frac{\partial \hat{\mathbf{x}}}{\partial \mathbf{x}} = (\mathbf{S}_a^{-1} + \mathbf{K}_i^T \mathbf{S}_\epsilon^{-1} \mathbf{K}_i)^{-1} \mathbf{K}_i^T \mathbf{S}_\epsilon^{-1} \mathbf{K}_i. \quad (7)$$

## 2.2 Forward Model

The forward model predicts the top-of-atmosphere microwave brightness temperatures that should be measured by the individual channels of a radiometer given knowledge of the relevant geophysical parameters of the ocean and atmosphere. The forward model used here is based on the physical surface emissivity and Radiative Transfer Model (RTM) described in Wentz and Meissner (2000). The RTM consists of an atmospheric absorption model for oxygen, water vapor and cloud liquid water and a sea surface emissivity model that determines the emissivity as a function of sea surface temperature, sea surface salinity, sea surface wind speed and direction. Few components have been adjusted with respect to Wentz and Meissner (2000). These include the wind directional signal of sea surface emissivity, which has been left out; and the fact that we only use the V- and H- polarizations for the 6.9, 10.7, 18.7, 23.8, 36.5 GHz channels.

## 2.3 OE set-up

The measurement vector,  $\mathbf{y}$ , used in our forward model consists of dual polarization observations (v-pol and h-pol) at the 5 lower frequencies: 6.9, 10.7, 18.7, 23.8, 36.5 GHz. Four geophysical parameters are considered to be the leading terms controlling the observed microwave brightness temperatures in the measurement situation (considering open-ocean only):



$$\mathbf{x} = (\text{WS}, \text{TCWV}, \text{TCLW}, \text{SST}), \quad (8)$$

where WS is the wind speed, TCWV is the integrated columnar atmospheric water vapor content, TCLW is the integrated (columnar) cloud liquid water content, and SST is the sea surface temperature.

The variation of the retrieved geophysical parameters is restricted by use of a priori information from NWP about the mean (a priori state) and covariances of the parameters. The covariance matrix of the geophysical parameters related to  $\mathbf{x}$  is fixed to:

$$\mathbf{S}_a = \begin{bmatrix} e_{WS}^2 & 0 & 0 & 0 \\ 0 & e_{TCWV}^2 & 0 & 0 \\ 0 & 0 & e_{TCLW}^2 & 0 \\ 0 & 0 & 0 & e_{SST}^2 \end{bmatrix} \quad (9)$$

with  $e_{WS} = 2$  m/s,  $e_{TCWV} = 0.9$  mm,  $e_{TCLW} = 1$  mm and  $e_{SST} = 0.50$  K. The uncertainties on the WS, TCWV and TCLW are best estimates based upon published validation results (see e.g. Dee et al., 2011; Chelton and Freilich, 2005; Jakobson et al., 2012; Li et al., 2008; Jiang et al., 2012). The SST uncertainty is derived from a comparison against Argo drifting buoys. The measurement covariance matrix,  $\mathbf{S}_\epsilon$ , is calculated from the differences between the observed and calculated TBs ( $\text{TB}_{\text{obs}} - \text{TB}_{\text{calc}}$ ). It is set to:

	6V	6H	10V	10H	18V	18H	23V	23H	36V	36H
6V	0.1162	0.1268	0.0412	-0.0286	0.0082	-0.1338	0.0843	-0.0531	0.1071	-0.0015
6H	0.1268	0.3069	-0.0340	-0.0689	-0.0689	-0.2258	0.0927	-0.0562	0.1590	0.0238
10V	0.0412	-0.0340	0.1181	0.0389	0.0982	-0.0243	0.0736	-0.0818	0.0788	0.0389
10H	-0.0286	-0.0689	0.0389	0.0903	0.0007	0.0336	-0.0187	-0.0411	-0.0146	0.0007
18V	0.0082	-0.0689	0.0982	0.0007	0.2283	0.0695	0.1010	-0.1069	0.1127	0.1001
18H	-0.1338	-0.2258	-0.0243	0.0336	0.0695	0.2816	-0.1257	0.0015	-0.1481	0.0215
23V	0.0843	0.0927	0.0736	-0.0187	0.1010	-0.1257	0.2706	-0.0278	0.2024	0.1039
23H	-0.0531	-0.0562	-0.0818	-0.0411	-0.1069	0.0015	-0.0278	0.2591	-0.1137	0.0009
36V	0.1071	0.1590	0.0788	-0.0146	0.1127	-0.1481	0.2024	-0.1137	0.2771	0.0935
36H	-0.0015	0.0238	-0.0389	-0.0007	-0.1001	-0.0215	-0.1039	-0.0009	-0.0935	0.0902

with matrix elements given in  $\text{K}^2$ . In order to calculate the Jacobians we use the disturbance parameter,  $\epsilon$ :

$$\epsilon = [0.2\text{m/s } 0.1\text{mm } 0.02\text{mm } 0.25\text{K}] \quad (10)$$

### 2.3.1 Iterations

According to Rodgers (2000) the most straightforward convergence test is to ensure that the cost function (Equation 4) is being minimized. The change in the cost function between two subsequent iterations will always be small near a cost minimum. Noting that the expected value of the cost function at the minimum is equal to  $m$  degrees of freedom ( $m=10$ ) an appropriate test would be to require the change between iterations of  $\Delta\mathbf{J} = \mathbf{J}_i - \mathbf{J}_{i+1} \ll m$  or  $\Delta\mathbf{J} = \mathbf{J}_i - \mathbf{J}_{i+1} < 0.1$ . In addition,  $\Delta\mathbf{J}$  is required to be positive at the final solution.

A maximum of 10 iterations are allowed and a failure to meet the above convergence criterion within 10 iterations will lead to an exclusion of the data (<0.1%). Usually, there are less than 6 iterations until the above criterion is met.

### 2.3.2 Bias corrections

In order to correct for the forward modelling error, we apply two bias corrections. The two step procedure was tested to be superior to the one step bias correction. In the first bias correction of the forward model the observed brightness temperatures are corrected by adding a constant to each channel:

$$TB_{bias} = \begin{matrix} & 6V & 6H & 10V & 10H & 18V & 18H & 23V & 23H & 36V & 36H \\ = & 0.3524 & 0.0793 & -0.1093 & -0.7521 & 0.6228 & 0.2794 & 0.0200 & -0.2669 & -0.3540 & 0.1464 \end{matrix}$$

We apply a second bias correction scheme using empirical fitting of simulated brightness temperatures minus observed brightness temperatures to analytic functions of SST, WS; and  $\varphi_r$ . The regression model obtained for the forward model residuals is:

$$a_1 + b_1SST + b_2SST^2 + c_1WS + c_2WS^2 + d_1 \cos(\varphi_r) + d_2 \sin(\varphi_r) + d_3 \cos\left(\frac{\varphi_r}{2}\right) + d_4 \sin^2\varphi_r + d_5 \cos^2\varphi_r + d_6 \sin^3\varphi_r + d_7 \cos^3\varphi_r + d_8 \sin^4\varphi_r, \quad (11)$$

with coefficients for each channel given in Table 1.

**Table 1.** Coefficients used for the empirical bias correction of the forward model.

	6V	6H	10V	10H	18V	18H	23V	23H	36V	36H
<b>a<sub>1</sub></b>	-2629	-0.043863	0.00092174	0.16561	-0.0037224	11.097	-0.07976	31.758	1031.09.00	-3585.5
<b>b<sub>1</sub></b>	-761.31	-0.046834	0.0015381	0.009931	0.0056594	32.557	0.55457	-22.138	300.19.00	-949.8
<b>b<sub>2</sub></b>	-1950.2	-0.0049384	-0.00045973	0.16759	-0.0075212	86.239	0.79548	-38.605	773.37.00	-2506.6
<b>c<sub>1</sub></b>	1318.03.00	0.0096035	-0.00076459	0.035344	-0.0043369	-48.318	29.678	-140.28	-502.2	2332
<b>c<sub>2</sub></b>	-1227.7	0.036307	-0.0011215	0.863194444	-0.0047699	54.553	12.112	-60.005	486.54.00	-1433.1
<b>d<sub>1</sub></b>	2719.05.00	0.04087	-0.00090555	0.032087	-0.0052348	-11.19	24.609	-117.12	-1062.8	4159.05.00
<b>d<sub>2</sub></b>	-3547.6	0.0056961	-0.0009869	0.0019303	0.0013516	13.986	-51.863	247.19.00	1372.04.00	-5784.8
<b>d<sub>3</sub></b>	-1442.1	0.01482	-0.00035264	-0.17036	0.0060634	39.163	-99.164	466.18.00	520.51.00	-3759.8
<b>d<sub>4</sub></b>	-2965.2	-0.0051674	-0.00014784	0.073759	-2.05E-01	11.966	14.513	-61.712	1153.04.00	-3771.1
<b>d<sub>5</sub></b>	2713.09.00	-0.0096709	0.00056282	-0.027147	0.0016354	-10.306	21.689	-102.28	-1041.5	4063.07.00
<b>d<sub>6</sub></b>	-2629	-0.043863	0.00092174	0.16561	-0.0037224	11.097	-0.07976	31.758	1031.09.00	-3585.5
<b>d<sub>7</sub></b>	-761.31	-0.046834	0.0015381	0.009931	0.0056594	32.557	0.55457	-22.138	300.19.00	-949.8
<b>d<sub>8</sub></b>	-1950.2	-0.0049384	-0.00045973	0.16759	-0.0075212	86.239	0.79548	-38.605	773.37.00	-2506.6

The second step bias correction is added to the simulated brightness temperatures individually, every time the forward model is called using retrieved SST and WS from the latest iteration.

### 2.3.2 Final configuration

Figure 1 illustrates the different processes performed in the final DMI OE algorithm. First the algorithm reads in the predefined  $S_\epsilon$ ,  $S_a$  and  $\epsilon$  values. The observation loop is started for each satellite observation pixel by reading the observed brightness temperatures and the first guess values. Afterwards the iteration process is initiated. For each iteration, the forward model is used to calculate the simulated brightness temperature from the state vector (in the first step: state vector = first guess values). Moreover, the Jacobians ( $K$ ), cost function ( $J$ ), uncertainty ( $S_x$ ) and sensitivity ( $A$ ) are calculated. The change in the cost function between two iterations is used to test for convergence and a maximum of 10 iterations are allowed. Until convergence is met, the state vector is updated for each



iteration step and the iteration continues. When the iteration process is stopped the state vector is saved together with the output data listed in the following section.

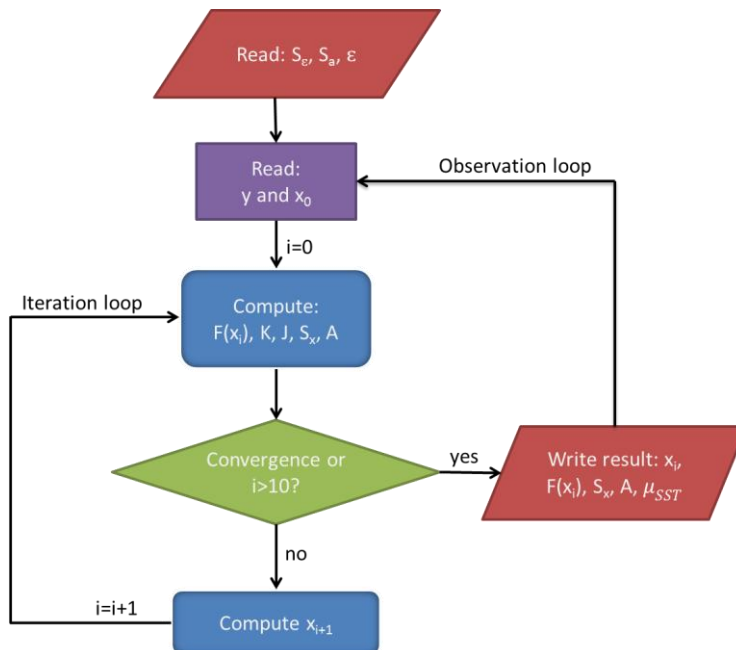


Figure 1. Flowchart of the DMI Optimal Estimation algorithm.

The OE methodology directly provides an estimate of the retrieval uncertainty,  $\mathbf{S}_x$ , due to uncertainties in the measurements, forward model, and in the a priori state vector (sees Equation 6). However, it is also found that the quality of the SST retrieval is closely connected to the root mean squared error of the simulated brightness temperatures minus observed brightness temperatures ( $RMSE_{TB}$ ). For that reason, we have set up an additional uncertainty indicator based on a scaled  $RMSE_{TB}$  value:

$$\mu_{SST} = 0.55 * RMSE_{TB} \quad (12)$$

with

$$RMSE_{TB} = \sqrt{\frac{1}{n} \sum_{i=1}^n (TB_{obs} - TB_{calc})^2}, \quad (13)$$

The scaling factor of 0.55 was found from comparison with *in situ* observations and under the assumptions that drifting buoys have a total uncertainty of 0.2 K and that the sampling uncertainty is 0.3 K.

## 2.4 Output data

When the convergence criterion has been met, the retrieval is finished. The outputs of the optimal estimation algorithm are; the retrieval state vector consisting of wind speed, total column water vapor, total cloud liquid water, and sea surface temperature; their uncertainties; corresponding averaging kernels; corresponding simulated brightness temperatures etc. for each AMSR-E measurement:

- Retrieved state vector:  $\mathbf{x}$
- Simulated brightness temperatures from final iteration:  $\mathbf{F}(\mathbf{x})$

- OE uncertainty:  $\mathbf{S}_x$
- SST uncertainty:  $\mu_{SST}$
- Averaging Kernels:  $\mathbf{A}$
- Observed brightness temperatures:  $\mathbf{y}$
- First guess (NWP):  $\mathbf{p}_0$  [WS, TCWV, TCLW, SST]
- Number of iterations performed:  $i$

## Appendix A

Table A1: Coefficients for the pressure calculation.

a	b
0.000000	0.000000
20.000.000	0.000000
38.425.343	0.000000
63.647.804	0.000000
95.636.963	0.000000
134.483.307	0.000000
180.584.351	0.000000
234.779.053	0.000000
298.495.789	0.000000
373.971.924	0.000000
464.618.134	0.000000
575.651.001	0.000000
713.218.079	0.000000
883.660.522	0.000000
1.094.834.717	0.000000
1.356.474.609	0.000000
1.680.640.259	0.000000
2.082.273.926	0.000000
2.579.888.672	0.000000
3.196.421.631	0.000000
3.960.291.504	0.000000
4.906.708.496	0.000000
6.018.019.531	0.000000
7.306.631.348	0.000000
8.765.053.711	0.000076
10.376.126.953	0.000461
12.077.446.289	0.001815
13.775.325.195	0.005081
15.379.805.664	0.011143
16.819.474.609	0.020678
18.045.183.594	0.034121
19.027.695.313	0.051690
19.755.109.375	0.073534
20.222.205.078	0.099675
20.429.863.281	0.130023
20.384.480.469	0.164384
20.097.402.344	0.202476
19.584.330.078	0.243933
18.864.750.000	0.288323
17.961.357.422	0.335155
16.899.468.750	0.383892
15.706.447.266	0.433963
14.411.124.023	0.484772



13.043.218.750	0.535710
11.632.758.789	0.586168
10.209.500.977	0.635547
8.802.356.445	0.683269
7.438.803.223	0.728786
6.144.314.941	0.771597
4.941.778.320	0.811253
3.850.913.330	0.847375
2.887.696.533	0.879657
2.063.779.785	0.907884
1.385.912.598	0.931940
855.361.755	0.951822
467.333.588	0.967645
210.393.890	0.979663
65.889.244	0.988270
7.367.743	0.994019
0.000000	0.997630
0.000000	1.000.000

## References

- Block, T., Embacher, S., Merchant, C. J., and Donlon, C.: High Performance Software Framework for the Calculation of Satellite-to-Satellite Data Matchups (MMS version 1.2), *Geosci. Model Dev. Discuss.*, <https://doi.org/10.5194/gmd-2017-54>, in review, 2017.
- Boyer, T.P., J. I. Antonov, O. K. Baranova, C. Coleman, H. E. Garcia, A. Grodsky, D. R. Johnson, R. A. Locarnini, A. V. Mishonov, T.D. O'Brien, C.R. Paver, J.R. Reagan, D. Seidov, I. V. Smolyar, and M. M. Zweng. 2013: *World Ocean Database 2013*, NOAA Atlas NESDIS 72, S. Levitus, Ed., A. Mishonov, Technical Ed.; Silver Spring, MD, 209 pp., <http://doi.org/10.7289/V5NZ85MT>
- Chelton, D. B., & Wentz, F. J. (2005). Global microwave satellite observations of sea surface temperature for numerical weather prediction and climate research. *Bulletin of the American Meteorological Society*, 86(8), 1097-1115.
- Chelton, D. B. & Freilich, M. H. (2005). Scatterometer-Based Assessment of 10-m Wind Analyses from the Operational ECMWF and NCEP Numerical Weather Prediction Models. *Mon. Weather Rev.*, 133, 409–429, doi:10.1175/MWR-2861.1.
- Dee, D. P., Uppala, S. M., Simmons, A. J., Berrisford, P., Poli, P., Kobayashi, S., Andrae, U., Balmaseda, M. A., Balsamo, G., Bauer, P., Bechtold, P., Beljaars, A. C. M., van de Berg, L., Bidlot, J., Bormann, N., Delsol, C., Dragani, R., Fuentes, M., Geer, A. J., Haimberger, L., Healy, S. B., Hersbach, H., Hólm, E. V., Isaksen, I., Kållberg, P., Köhler, M., Matricardi, M., McNally, A. P., Monge-Sanz, B. M., Morcrette, J.-J., Park, B.-K., Peubey, C., de Rosnay, P., Tavolato, C., Thépaut, J.-N. and Vitart, F. (2011), The ERA-Interim reanalysis: configuration and performance of the data assimilation system. *Q.J.R. Meteorol. Soc.*, 137: 553–597. doi: <http://dx.doi.org/10.1002/qj.828>
- Donlon, C., Rayner, N., Robinson, I., Poulter, D. J. S., Casey, K. S., Vazquez-Cuervo, J., ... & May, D. (2007). The global ocean data assimilation experiment high-resolution sea surface temperature pilot project. *Bulletin of the American Meteorological Society*, 88(8), 1197-1213.
- Donlon, C., Casey, K., Gentemann, C., LeBorgne, P., Robinson, I., Reynolds, R., ... & Cornillon, P. (2009). Successes and challenges for the modern sea surface temperature observing system. *Community White Paper for OceanObs*, 9.
- Good, S. A., M. J. Martin and N. A. Rayner. (2013). EN4: quality controlled ocean temperature and salinity profiles and monthly objective analyses with uncertainty estimates, *Journal of Geophysical Research: Oceans*, 118, 6704-6716, doi:10.1002/2013JC009067
- Jakobson, E.; Vihma, T.; Palo, T.; Jakobson, L.; Keernik, H.; Jaagus, J., 2012. Validation of atmospheric reanalyses over the central Arctic Ocean: TARA REANALYSES VALIDATION. *Geophys. Res. Lett.* 39, doi:10.1029/2012GL051591.
- Jiang, J. H.; Su, H.; Zhai, C.; Perun, V. S.; Del Genio, A.; Nazarenko, L. S.; Donner, L. J.; Horowitz, L.; Seman, C.; Cole, J.; Gettelman, A.; Ringer, M. A.; Rotstayn, L.; Jeffrey, S.; Wu, T.; Briant, F.; Dufresne, J.-L.; Kawai, H.; Koshiro, T.; Watanabe, M.; LÉcuyer, T. S.; Volodin, E. M.; Iversen, T.; Drange, H.; Mesquita, M. D. S.; Read, W. G.; Waters, J. W.; Tian, B.; Teixeira, J.; Stephens, G. L., 2012. Evaluation of cloud and water vapor simulations in CMIP5 climate models using NASA "A-Train" satellite observations: EVALUATION OF IPCC AR5 MODEL SIMULATIONS. *J. Geophys. Res. Atmospheres*, 117, doi:10.1029/2011JD017237.
- Li, J.-L. F.; Waliser, D.; Woods, C.; Teixeira, J.; Bacmeister, J.; Chern, J.; Shen, B.-W.; Tompkins, A.; Tao, W.-K.; Köhler, M., 2008. Comparisons of satellites liquid water estimates to ECMWF and GMAO analyses, 20th century IPCC AR4 climate simulations, and GCM simulations. *Geophys. Res. Lett.*, 35, doi:10.1029/2008GL035427.
- McPhaden, M. J., et al. (2009), The Global Tropical Moored Buoy Array, paper presented at OceanObs'09 Conference - Sustained Ocean Observations and Information for Society, ESA, Venice, Italy, 21-25 September 2009
- Merchant, C. J., P. Le Borgne, H. Roquet, and G. Legendre (2013), Extended optimal estimation techniques for sea surface temperature from the Spinning Enhanced Visible and Infra-Red Imager (SEVIRI), *Remote Sensing of Environment*, 131, 287-297, doi:<http://dx.doi.org/10.1016/j.rse.2012.12.019>.

- Nielsen-Englyst, P., Høyer, J. L., Pedersen, L. T., Gentemann, C., Alerskans, E., Block, T. & Donlon, C. (2018). Optimal estimation of sea surface temperature from AMSR-E, Remote Sensing (in press).
- Reynolds, R. W. (1993). Impact of Mount Pinatubo aerosols on satellite-derived sea surface temperatures. *Journal of climate*, 6(4), 768-774.
- Reynolds, R. W., Rayner, N. A., Smith, T. M., Stokes, D. C., & Wang, W. (2002). An improved in situ and satellite SST analysis for climate. *Journal of climate*, 15(13), 1609-1625.
- Rodgers, C.D. (2000), *Inverse methods for atmospheric sounding. Theory and practice*, World Scientific, Singapore.
- Vazquez-Cuervo, J., Armstrong, E.M., Harris, A. (2004). The effect of aerosols and clouds on the retrieval of infrared sea surface temperature. *Journal of climate*, 17 (20), 3921–3933, 2004.
- Wentz, F. J., Gentemann, C., Smith, D., & Chelton, D. (2000). Satellite measurements of sea surface temperature through clouds. *Science*, 288(5467), 847-850.
- Wentz, F. and T. Meissner. 2000. AMSR Ocean Algorithm. Algorithm Theoretical Basis Document, Version 2. Santa Rosa, California USA: Remote Sensing Systems.
- Zweng, M. M, J. R. Reagan, J. I. Antonov, R. A. Locarnini, A. V. Mishonov, T. P. Boyer, H. E. Garcia, O. K. Baranova, C. R. Paver, D. R. Johnson, D. Seidov, M. Biddle, 2013: *World Ocean Atlas 2013, Volume 2: Salinity*. S. Levitus, Ed., A. Mishonov, technical editr, NOAA Atlas NESDIS 74.'